Break-up of Continuous Liquid Jets: Effect of Nozzle Geometry

B. Lopez, A. Soucemarianadin*,† and P. Attané

Laboratoire de Rhéologie, CNRS and Univ. J. Fourier, Cedex, France

In this article we present the results obtained on jet break-up using two types of nozzles having the same nozzle aspect ratio but exhibiting different entry and exit holes. To further emphasize the effect of nozzle geometry, we use two different stimulations of the jet, respectively a piezoelectric transducer located upstream the orifice and an ElectroHydroDynamic (EHD) exciter that consists of an electrode situated downstream from the nozzle. The different measurement techniques used are essentially a stroboscopic illumination of the jet and a laser photometry method. These two methods allow us to obtain information on both the break-up lengths and the spatial evolution of the jet shape. Spectral analysis combined with the laser photometric method shows the evolution of Fourier amplitudes of the jet radius and phase shifts between the fundamental and the harmonics for low and high initial perturbations. In particular, this method reveals drastic differences between nozzles that may be ascribed to the drop formation behavior of jets.

Journal of Imaging Science and Technology 43: 145–152 (1999)

Introduction

Continuous ink-jet printing largely relies on the production of uniformly sized and charged droplets caused by the break-up and charging of a periodically disturbed jet. Generally to make the break-up repeatable, the jet is submitted to a disturbance introduced by a transducer.

The parameters controlling the break-up of fluids are its physico-chemical properties (e.g., surface tension, viscosity) and mechanical effects such as velocity. Also of considerable importance are the amplitude and type of the excitation signal[1,2] and the nozzle geometry that has been overlooked until now except for the work by McCarthy and Molloy.[3] However these authors limit their investigation to the main geometrical factors influencing the velocity profile at the orifice exit and do not give details in their paper as to the method of evaluating the performances of different types of nozzles.

If an ink jet printer is to work properly and reliably, it must be fitted with nozzles that are able to produce drops at a stable and repeatable frequency, be insensitive to small variations in fluid parameters and operating conditions, and give the shortest break-up length possible at the lowest excitation voltage. To decide if a nozzle is working appropriately, the drops are usually viewed under stroboscopic illumination but this technique alone often proves insufficient.[4] Moreover, to discriminate between different types of nozzles it is necessary to obtain quantitative information on capillary wave dynamics that control jet break-up.

In this article, we report results obtained for two types of nozzles using both the stroboscopic technique for measuring break-up lengths and a laser photometric method that has been shown to be adequate for non-intrusive measurements of the jet surface profile.[5] Spectral analysis is used in conjunction with the laser photometric method to process the signals to recover the amplitudes of different Fourier modes and phase shifts of harmonics relative to the fundamental. This enables us to pinpoint the differences in development of an initial disturbance applied to a jet issuing from a given type of orifice and thus, propose a method capable of evaluating in a quantitative manner, nozzle performances in terms of jet break-up.

Original manuscript received April 9, 1998

* IS&T Member

† Corresponding author, e-mail: souce@ujf-grenoble.fr

Background

The role of orifice geometry has seldom been considered in the case of capillary pinching (also called Rayleigh instability mode) which is the dominant mechanism of jet break-up in continuous ink-jet applications.

McCarthy and Molloy[3] attempted to form a qualitative correlation between the nozzle configuration and issuing jet shape. They were mainly interested in studying the efficient conversion of potential energy to kinetic energy and the effect of the nozzle aspect ratio L/D on the initial jet velocity profile and subsequent jet shape.

Other studies relevant to the role of orifice flow patterns on jet break-up have been carried out in the domain of fluid atomization where the Taylor instability mode prevails. In this field, researchers have essentially varied nozzle aspect ratios[6] to change the internal structure of the core that controls the droplet size and velocity.

Our work differs in at least four aspects from others usually found in the literature:

a. We study the influence of nozzle entrance configurations while other researchers have mainly emphasized the effects of orifice aspect ratio L/D.
b. We report results on a jet exiting from nozzles having different entrance configurations and submitted to the superimposition of a sinusoidal perturbation on a steady flow. Other works concentrate mainly on steady flow.
c. We provide results on the continuous evolution of the free surface from nozzle exit to jet break-up using a

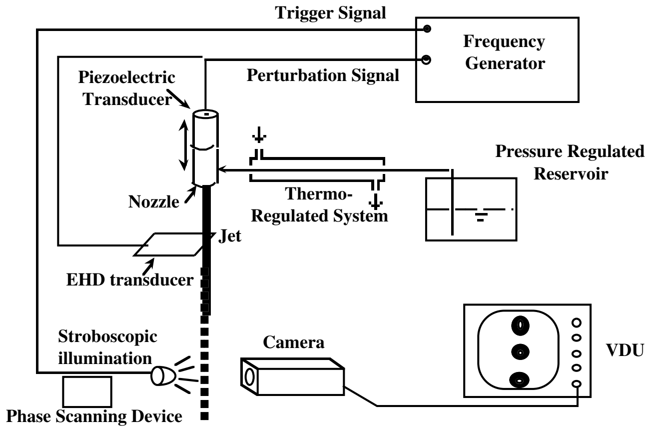

Figure 1. Schematic of the experimental set-up.

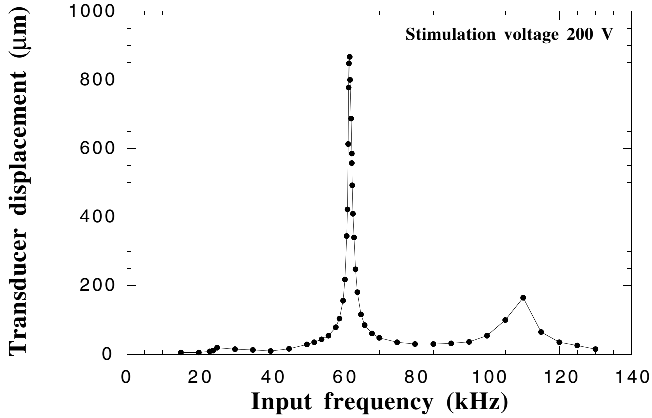

Figure 2. Transducer displacement as a function of frequency.

specifically developed set-up. Other works are limited to the measurements of global parameters such as break-up lengths or drop sizes.

d. We pinpoint differences between nozzles at both low and high initial perturbations. This important aspect has not been taken into account in previous works.

Experimental

The different stimulation devices and measurement methods used in this study are presented in detail. In particular, we characterize the piezoelectric tranducer over a large range of frequencies. We also discuss the different technologies that may be used to manufacture nozzles for ink-jet applications.

Jet Generation and Stimulation

In this study, we have used either a piezoelectric stimulation technique[7] or an ElectroHydroDynamic (EHD) method[8] to impose a periodical disturbance onto the jet issuing from a nozzle. Temperature controlled fluid is supplied from a nitrogen pressure-regulated reservoir to the fluid chamber. Typical pressures used are of the order of 0.4 MPa. The fluid is carefully filtered and flushed through the supply line before starting the jet. The vertical jet issues from the nozzle where length over diameter ratio is of the order of 1. The diameter of the jet is roughly equal to that of the nozzle for the different types of nozzles used in this investigation and the mean diameter of the jets is 70 mm. Other details are shown in Fig. 1.

The piezoelectric stimulation technique essentially consists of a fluid chamber comprising a resonator at one end and a nozzle at the other. The resonator is made of a piezoelectric ceramic bonded to a steel rod. The expansion and contraction of the piezoceramic-rod assembly within the fluid chamber helps to create the initial disturbance in the form of a velocity perturbation that is then amplified along the jet and leads to drop break-up. Jet break-up either in presence or absence of satellites could be obtained by this technique as demonstrated in the results section. The displacement of the transducer as a function of frequency is shown in Fig. 2 for an excitation voltage of 200 V. This result has been obtained at ambient pressure using a vibrometer (Polytec OFV-2601, Germany) that measures surface motion using interferometric techniques. Note that the resonant frequency under these conditions is between 62 and 63 kHz, while the harmonic is around 110 kHz. There may be a slight shift in resonant frequency and probably also a change in the amplitude of vibration when the transducer is submitted to pressure (under flow conditions) but the overall behavior should remain the same.

The EHD stimulation method used in this study consists of a simple electrode (a thin metallic foil of 60 mm in thickness) that is located near the jet with a clearance of the order of 20 mm (see Fig. 1). In contrast to the piezoelectric stimulation technique, this method that induces a radial perturbation onto the jet can only generate drops interspersed with slow satellites. Indeed as shown in the next section, this type of stimulation is more than two orders of magnitude less efficient than piezoelectric excitation, so other disturbance waveforms have to be found[9] to eliminate these satellites.

A frequency function/amplifier generator (Hewlett Packard 3245A, USA) is used to drive either the piezoelectric crystal or the EHD electrode with a periodically varying voltage comprised between 1 and 200 Volts peak-to-peak (Vpp). A laboratory manufactured built amplifier allows us to obtain voltages up to 600 Vpp when using the EHD perturbation method. The amplitude and frequency of the function generator are manually operated. This generator also drives at the same frequency as the transducer, a pulsed light emitting diode (LED) that helps to capture still images of jet break-up using a CCD camera (Watec, USA) coupled with a zoom allowing for a magnification of about 10. The exposure times are on the order of 0.5 ms. A phase scanning device set between the generator and the LED allows us to introduce a variable phase shift between the transducer triggering signals and those of the LED[7] and thus has a resolution of 1/8 of the wavelength (around 30 µm) in terms of break-up length measurements.

Nozzle Configurations

A number of nozzle manufacturing technologies can be found in the literature. Hershberg and co-workers[10] proposed using micro-punching and/or microelectric discharge machining. Kitahara[11] fabricated nozzles in a stainless steel foil using etching technology whereas Endert and coworkers[12] found that excimer laser micromachining was an excellent tool for precision manufacturing.

In our study, we have used two nozzle set-ups that have been manufactured using some of the above cited technologies (Fig. 3). They present the same aspect ratio L/D of one and differ by their entrance and exit geometries. Nozzle set-up (A) consists only of a cylindrical section having a diameter of 70 µm while nozzle set-up

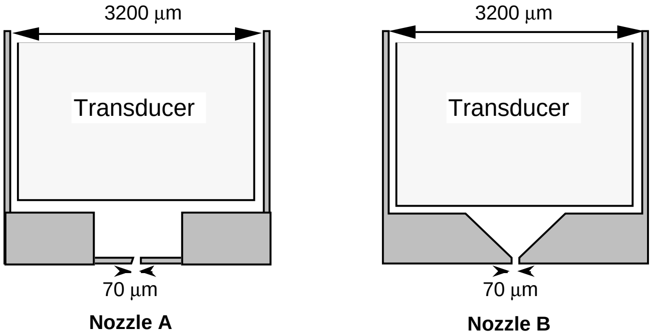

Figure 3. Schematic of different nozzle shapes.

(B) combines both cylindrical and tapered sections. Our objectives in this work are to find the nozzle offering the highest efficiency in terms of stimulation (i.e., the shortest break-up length together with the lowest excitation voltage) and to understand the physical reasons underlying the phenomenon of jet instability.

Fluid Properties

To be sure that the effects identified were due to differences in nozzle geometries only, we confirmed the fluid that was used in all our experiments was purely Newtonian over a large range of shear and deformation rates using different methods that are described elsewhere.[13] The ink had a viscosity η of 4.4 mPa.s, a density ρ of 1172 kg/m^3, a static surface tension σ_s of 50 mN/m and a conductivity of 2500 μS/cm which is amply sufficient for using the EHD excitation method.

Laser Shadow Method

This method allows us to perform non-intrusive measurements of the jet surface profile. This extremely accurate technique that has the capability to resolve relative diameter variations as small as 5.10^{-3} has been discussed in an exhaustive manner elsewhere[5] and therefore only the main features necessary for the understanding of the results given in the next section will be presented here.

Components of the measuring system are a laser diode and attendant optics that shape the beam into a thin laser sheet. A spherical lens where location can be varied according to the desired magnification factor (25 to 40) is also positioned behind the jet. In the course of the experiment the dyed fluid jet that is opaque is scanned from the nozzle to the break-up point using a motorized micro-positioner stage where the drop generation system is installed. The entire device including the translation stage, necessary optics, and detection means are mounted on a heavy granite optical table with self-levelling supports for vibration isolation.

The transmitted light that gives the jet profile passes through a diaphragm and a slit before being focused by a lens and projected onto a photodiode. The signal collected by the photodiode is amplified before being sampled using a digital oscilloscope (Nicolet 4180, USA). An averaging technique improves the signal over noise ratio.

A Discrete Fourier Transform (DFT) procedure is used to expand the jet radius into Fourier modes and to extract information on both amplitudes of different modes and phase shifts between the fundamental and the harmonics of the jet radius that can be written accordingly:

$$R(z,t) = A_o + \sum_{n=1}^{N} A_n(z)\cos\left(n\left(2\pi ft - \frac{2\pi}{\lambda}z\right) + \phi_n(z)\right) \quad (1)$$

The number of Fourier modes considered is variable and depends on the initial perturbation i.e., on the excitation voltage. Indeed as we shall see later on, few modes can be sufficient to describe the spatial evolution of the jet at small amplitudes of the excitation voltage, while more modes are required as the jet becomes increasingly non-linear.

Results and Discussion

Break-up length measurements are performed at different excitation voltages using two types of nozzles. This allows us to characterize the efficiency in terms of stimulation for both nozzles. Then tests are conducted using the laser shadow method. The data obtained gives the initial disturbance input to the jet and provides relevant information as to the differences between nozzles.

Disturbance Growth and Fluid Dynamics

Before going into the details of this study, it is necessary to recall the basic relationships of the break-up of a liquid jet within the framework of linear stability analysis. Typically, controlled instability of a fluid stream is introduced by perturbing the jet with a sinusoidal waveform although other forms of disturbances have been considered.[1,2,9]

For our purposes, we consider an axisymmetric jet issuing from a nozzle of radius R_0. The jet travels at a velocity v_0 (of the order of 20 m/s) which is much greater than the characteristic capillary speed $v_c = (\sigma/\rho d)^{1/2}$ and may be perturbed using different methods with a frequency f of wavelength λ.

Rayleigh[14,15] developed the first linear stability analysis where he considered an infinite jet (inviscid[14] or viscous[15]) subject to a temporal disturbance growth. He showed that surface waves grow exponentially in time as $e^{\beta t}$. In a subsequent study the temporal growth rate β was given by Weber[16] for a viscous fluid with aerodynamic interactions.

To be exact, one should consider a spatio-temporal disturbance for the jet break-up problem at hand because the jet is finite with a nozzle at one end but Keller and co-workers[17] have demonstrated that both analyses agree for $v_c << v_0$. In our case v_c, is on the order of 1 m/s which is about 20 times smaller than v_0 so a temporal analysis is justified.

Break-up Length Measurements

If we assume that the linear analysis as given by Rayleigh is valid for the full jet then break-up is obtained when the perturbation is equal to the initial radius. If we assume further that the initial disturbance is proportional to the excitation voltage then the break-up length plotted versus the logarithm of the excitation voltage should be linear:

$$b = -\frac{\Delta Ln(V)}{\Delta L_b} \quad (2)$$

The spatial growth rate b can thus be obtained from the slope of the curve of the break-up length versus the logarithm of the excitation voltage and b is related to β through the following relationship: $\beta = bv_0$

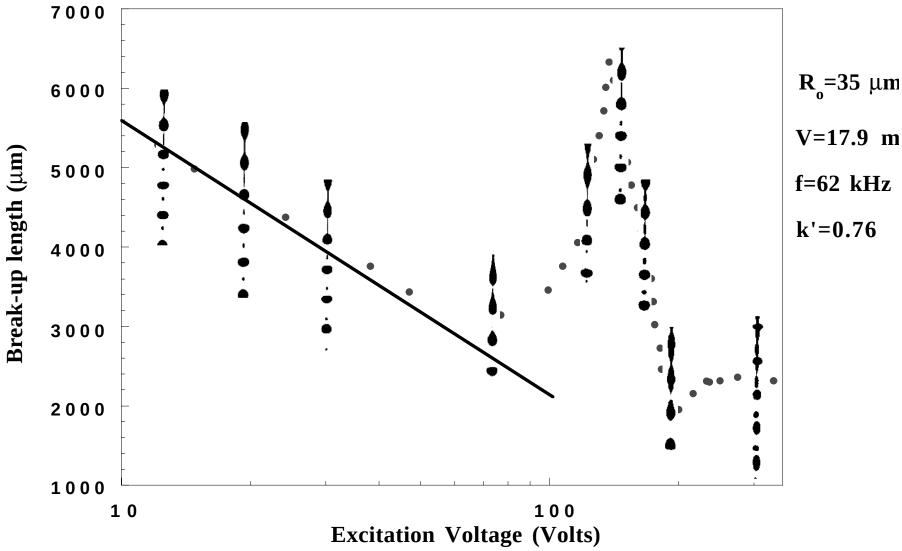

Figure 4. General map of jet break-up behaviour as a function of excitation voltage.

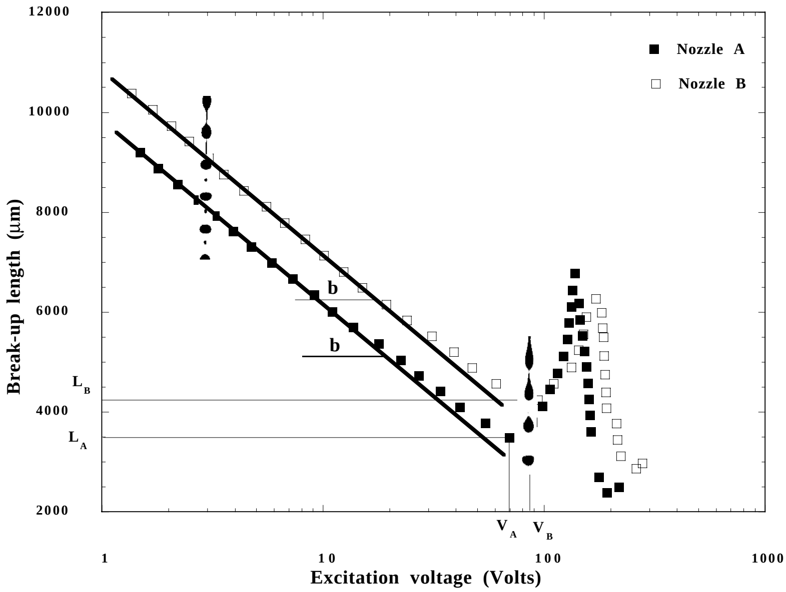

Figure 5. Break-up length measurements for two types of nozzles.

We obtain results very close to predictions up to a voltage of around 80 V if we refer to Fig. 4 where the tests have been performed for a jet velocity of 17.9 m/s, an excitation frequency of 62 kHz and a dimensionless wavenumber $k' = 2\pi R_0/\lambda$ of 0.76. Beyond that voltage, the non-linearities lead very different behaviors in terms of break-up distances as demonstrated in Fig. 4.

Also shown in Fig. 4 as inserts, are the stroboscopic photos of jets obtained for different voltages. First, we find the usual succession of jet break-ups beginning with a slow satellite (lowest excitation voltage) and ending with a stream of drops devoid of satellite at the first minimum in break-up length (intermediate voltages give successive break-up with an infinite satellite and with a fast satellite). This first zone is the one of interest in ink-jet printing and will be considered in detail in this work. By performing measurements at higher voltages, we have discovered a variety of jet break-ups with satellites of different sizes that are given in the figure for the sake of interest. Nevertheless, the explanations related to these different break-ups are well beyond the scope of discussion of this article.

Effect of Nozzle Geometry

To study the effect of the nozzle geometry, we have performed break-up length measurements using the two types of nozzles mentioned previously and the piezoelectric stimulation technique.

Referring to Fig. 5, we can see that the slopes are the same for both types of nozzles which is consistent with the fact that the growth rate does not depend on the

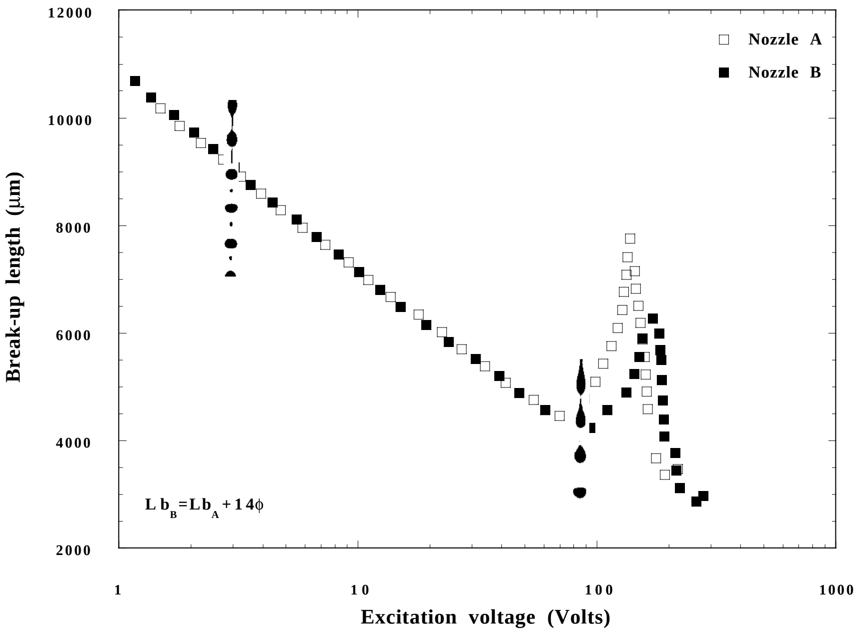

Figure 6. Superimposition of the break-up length measurements obtained for two different nozzle configurations.

type of nozzle that is used to perform the experiments. Nevertheless, the break-up lengths for the jets issuing from these nozzles are different for one given voltage. The slope that is calculated considers only data obtained for voltages smaller than 10 V because the linear analysis is only valid for small initial pertubations. Indeed we note in Fig. 5, that the slope is modified if all the data points (1 to 200 V) are taken into account.

If we consider the overall performances of the nozzles, we can attribute a higher efficiency factor to nozzle (A) compared to nozzle (B). As seen in Fig. 5, for a given break-up length of the jet, the excitation voltage is lower when using nozzle (A). Moreover, nozzle (A) allows us to have shorter break-up lengths. If we now refer to Fig. 3, we notice that the transducer is at the same distance from the nozzle outlet for both configurations. Because the break-up distance is different, we can hypothesize that this is due to the transition from a more or less parabolic profile to a flat one. Indeed if we follow Leib and Goldstein,[18] they show that the initial perturbation can only be amplified once the velocity profile effects have ceased. Figure 6 shows that the break-up lengths for nozzles (A) and (B) superimpose when a length of 14 diam (approximately 1 mm) is added (vertical shifting) to the break-up length of nozzle (A). This indicates that the inlet geometry of nozzle (B) induces a parabolic profile and has a large effect on the dynamics of jet break-up even for low amplitudes of the excitation voltage. We also note in Fig. 6, that the superimposition with only a vertical shifting is not valid at high excitation voltages. A master-curve can only be obtained by using both vertical and horizontal shiftings. Presently, this cannot be totally explained and further experiments are needed to clarify this point.

Low Initial Disturbance Experiments

In this section we perform experiments using both the piezoelectric and the EHD stimulation devices.

The objective is to evaluate the influence of the nozzle as harmonics are introduced into the jet, so we have performed tests to obtain the same break-up length that is indicated by the vertical line in Fig. 7. We have used nozzle (A) for this series of experiments which presents the highest efficiency. Under these conditions, for obtaining a break-up length (z/λ around 35) we used respectively 1 V for the piezoelectric excitation and 410 V for the EHD stimulation signal, as stated in the previous, section we find effectively a ratio of more than two orders of magnitude between the two types of stimulation.

The main advantage of EHD stimulation that is used in this work is its insensitivity to nozzle configurations because the electrode can be set at a location where velocity profiles should have relaxed, i.e., typically at around 700 μm (10 diam) underneath the orifice. This value is taken as 0 on the horizontal axis (Fig. 7) for the EHD measurements.

For the sake of legibility, only the amplitudes of the fundamentals (Fund. piezo and Fund. EHD) and the first two harmonics (respectively the second and the third) are reported in Fig. 7. As seen in the figure there is no real difference in terms of evolution of amplitudes at least to first-order between the disturbance input upstream the nozzle (piezoelectric excitation) and the excitation far downstream the nozzle (EHD). We conclude that velocity profile effects are probably almost absent for low initial disturbances for this orifice configuration. The slope of the fundamental that is given in Fig. 7 is equal to the spatial growth rate b due to Rayleigh's analysis, therefore we can write in the spatio-temporal frame, the radius R as:

$$R = R_0 + \varepsilon_0 e^{i(2\pi ft - kz)} e_{bz} \quad (3)$$

The growth of the fundamental is very close to exponential as expected from linear theories and from Eq. 3, we can calculate the temporal growth rate β and the dimensionless growth rate

$$\beta' = bV\sqrt{\frac{\rho {R_0}^3}{\sigma}}$$

where σ is the surface tension and R_0 is the radius of the nozzle. This is useful for comparison purposes with linear theories.

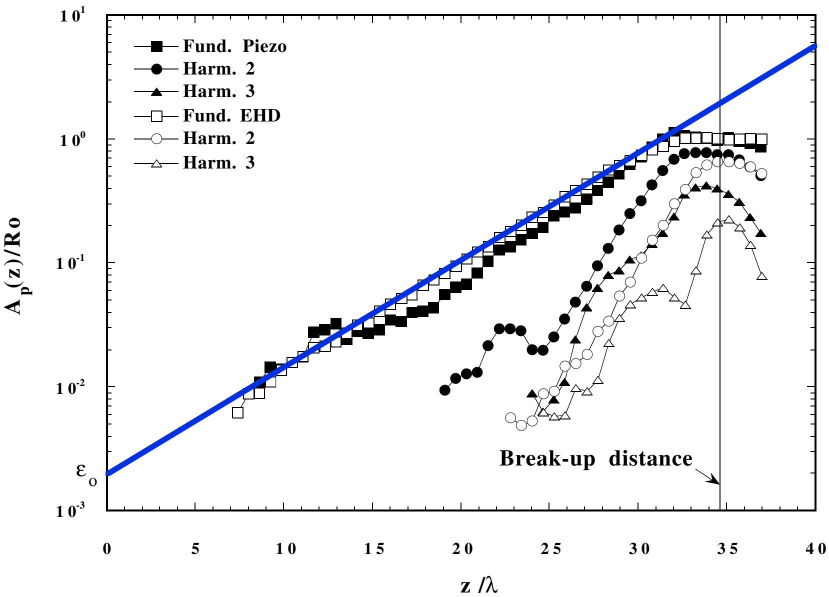

Figure 7. Normalized amplitudes for the fundamental and the first two harmonics when using piezoelectric and EHD stimulations.

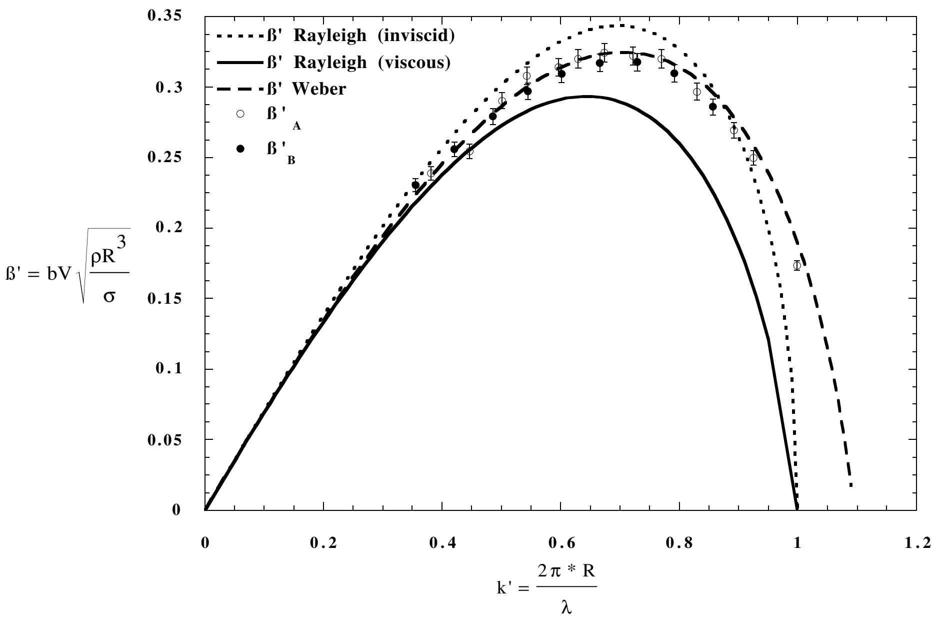

Figure 8. Comparisons between experimental data and different linear theories.

This is shown in Fig. 8 where we have plotted the data points obtained using different experimental methods and the curves that are the solutions of the various theoretical dispersion equations. Taub[19] for example has reported that an averaged normalized growth curve agreed well with the Rayleigh's inviscid theory.[14] This type of comparison is inappropriate because the fluid used in the experiments always has a finite viscosity. When compared to either the inviscid theory[14] results or to Rayleigh's viscous predictions,[15] our data presents a large discrepancy. Note that we have to take into account the aerodynamic effects i.e., Weber's modification[16] to considerably improve the agreement between experiments and theory. This indicates that the still ambient air contributes to an enhanced instability of the liquid jet.

High Initial Disturbance Experiments

As mentioned in the experimental section, the EHD stimulation is not sufficiently efficient to input a high initial disturbance onto the jet, so the experiments described in this section have been performed using the piezoelectric transducer.

The excitation voltage was 69 Vpp for the experiment conducted with nozzle (A) and 89 Vpp for the experiment performed with nozzle (B). This is due to the fact that we wanted to conduct the experiments at the minimum break-up length for both nozzles and as shown on Fig. 5; this leads to a lower excitation voltage for nozzle (A). The results obtained for the amplitudes and phase shifts are shown respectively in Figs. 9 and 11 [on both figures, open symbols are used for nozzle (A) and solid symbols for nozzle

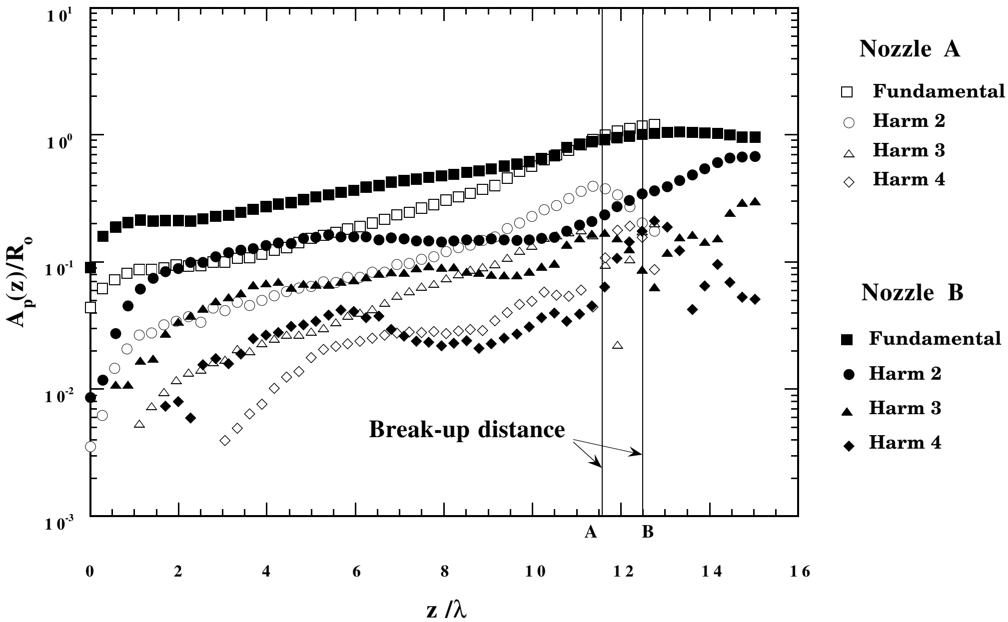

Figure 9. Normalized amplitudes of the different Fourier modes for experiments performed at high voltage using the two types of nozzles.

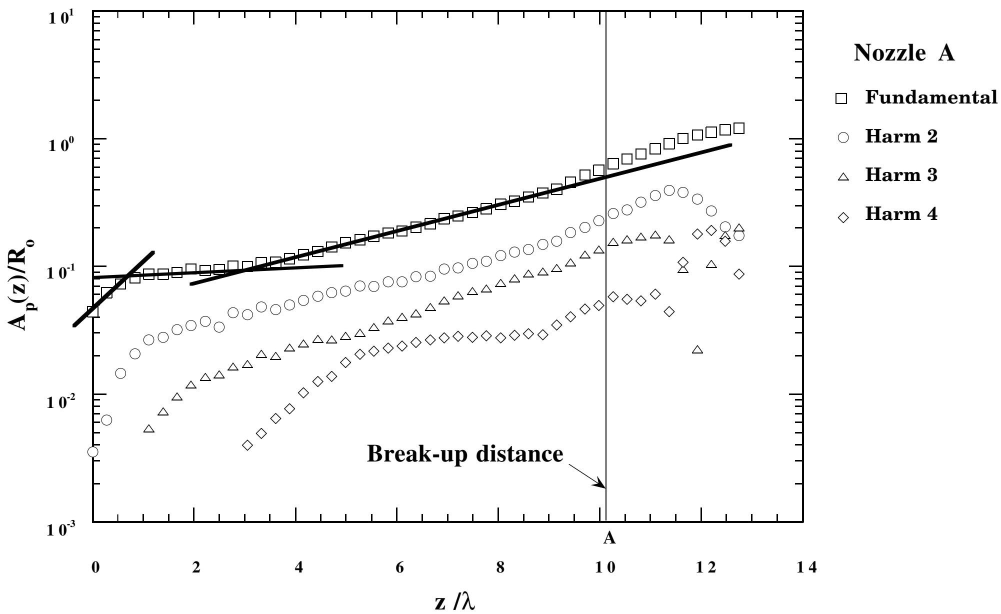

Figure 10. Normalized amplitudes of the different Fourier modes for experiments performed at high voltage using nozzle (A). Note the differences in slopes for the three régimes.

(B)]. In Fig. 7, the vertical lines indicate the break-up distances for the jets using these nozzles.

In this high initial disturbance regime, which is of practical use in ink-jet printing with a short break-up length, the jet behaviors are seen to be quite different for both types of nozzles (see Fig. 9). The growth of the amplitude of the fundamentals are far from being exponential all along the jet and, in contrast to the low initial disturbance regime results, higher harmonics are present right from the exit of the nozzles. As discussed by Fagerquist,[20] we demonstrate here, that once the initial disturbance becomes large, then the linear theory given by Rayleigh[15] does not apply, because the periodic perturbation is no longer monochromatic but described as a multi-frequency component.

Concerning the amplitude of the fundamental in the case of the jet issuing from nozzle (B), one can observe a plateau. For this experiment, the amplitude of the second harmonic initially grows, then stabilizes and begins to grow again. Similar behavior is also observed with other overtones. It seems that during the first part of the jet length ($z/\lambda < 2$) other effects probably vorticity seem to dominate over capillary instability, so for the high initial disturbance experiments there is an intricate mixing of kinematic and capillary effects. The practical consequence of this mixing is that jet break-up is delayed. This delay is much more important for the jet issuing from nozzle (B) than the one from nozzle (A). Further experiments still need to be performed to understand why kinematic effects are more amplified for

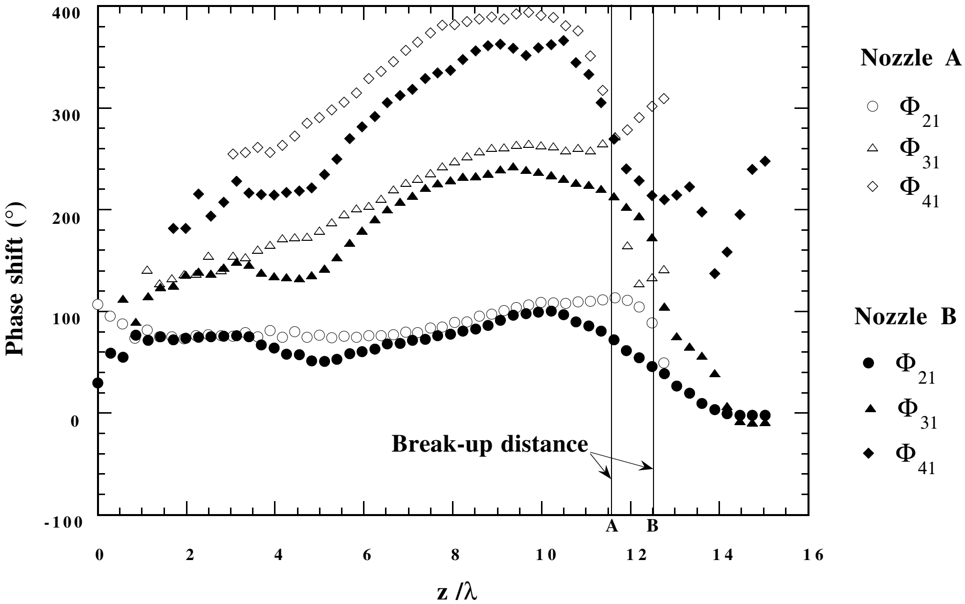

Figure 11. Phase shifts between the various Fourier modes for experiments performed at high voltage using the two types of nozzles.

one geometrical configuration compared to another.

In Fig. 10, we have plotted the dimensionless amplitudes of the first few Fourier modes (1 through 4). The results shown are for nozzle (A). We find that the growth of the fundamental can be broken up into three regimes, each of them represented by a straight line of different slope. The first regime with the highest slope is representative of the initial behavior of the jet where the perturbation tends to be greatly amplified. This is followed by a second regime where competitive effects (kinematic and capillary) seem to take place because the perturbation is almost stabilized. Finally we find a third zone with a growth rate that is smaller than what one would expect if only capillary effects were dominant. There is probably an interaction between the different modes since we find more or less the same behavior for the other modes.

Finally concerning the phase shifts (Fig. 11), note that close to the nozzle ($z/\lambda = 0$) there is a large difference for ϕ_{21} (equal to 110° for the jet issuing from nozzle (A) and 30° for (B) which is the phase shift between the fundamental and the second harmonic. In our opinion, this initial value can be assumed to be a characteristic of the nozzle and its flow geometry. This difference seems to subside slowly, and along the major part of the jet ϕ_{21} is equal to 80°. However the initial difference in phase shift leads to two different jet profiles and consequently to jet break-up behaviors that are not similar.

Conclusions

The role of the nozzle geometry on the break-up of liquid jets has been experimentally demonstrated in this article. For our purpose we have used two types of jet stimulation and various measurement methods.

The break-up length measurements performed with a stroboscopic illumination permits us to obtain efficiency values for different types of nozzles, but are not able to provide any information on capillary wave dynamics.

The laser shadow technique used in conjunction with DFT analysis allows us to extract values of the amplitudes and phase shifts of harmonics from the temporal variation of the jet radius. This method proves to be invaluable in characterizing the intricate surface phenomena and in pinpointing subtle differences between nozzles.

To summarize, our study leads us to conclude that in the low initial disturbance zone, nozzle differences begin to appear through what we think to be velocity profile effects and they become predominant for high initial perturbations which is of interest in most industrial applications.

Acknowledgements. The authors wish to thank Toxot Science and Applications for partial funding and in addition A. Soucemarianadin acknowledges support when working on this aspect within Toxot Science and Applications. This work has also been funded by the Ministère de l'Enseignement Supérieur, de la Recherche et de la Technologie through grant No. 92 P 0645. Finally the authors extend their appreciation to the Région Rhone-Alpes for partially funding this research under the EMERGENCE program and for financially supporting B. Lopez PhD thesis work through a research grant.

References

1. K. C. Chaudhary and T. Maxworthy, *J. Fluid Mech.* **96**, 275 (1980).
2. M. Orme and E.P. Muntz, *Phys. Fluids A* **2** (7) 1124 (1990).
3. M. J. McCarthy and N. A. Molloy, *Chem. Eng. Journal* **7**, 1 (1974).
4. L. Palm and J. Nilsson, *IS&T's 11th Intl. Cong. on Advances in Non-Impact Printing Technol.*, IS&T, Springfield, VA, 1995, p. 359.
5. J. Xing, A. Boguslawski, A. Soucemarianadin, P. Atten and P. Attané, *Exp. in Fluids* **20**, 302 (1996).
6. Z. Huang, Y.M. Shao, S. Shiga, H. Nakamura and T. Karasawa, *Proc. ICLASS 94.*
7. A. Badea, A. Dunand, A. Soucemarianadin and C. Carasso, *IS&T's 9th Intl. Cong. on Advances in Non Impact Printing Technol.*, IS&T, Springfield, VA, 1993, p. 256.
8. A. Spohn, P. Atten and A. Soucemarianadin, *Proc. IS&T's 9th Intl. Cong. on Advances in Non Impact Printing Technol.,* IS&T, Springfield, VA, 1993, p. 294.
9. B. Barbet, P. Atten and A. Soucemarianadin, *J. Imaging Sci. Technol.* **41**, 570 (1997).
10. E. Hershberg, G. Beenen, B. Boso, P. Krein, R. Marantz and B. Murdock, *J. Imaging Technol.* **14**, 124 (1988).
11. T. Kitahara, *IS&T's 11th Intl. Cong. on Advances in Non Impact Printing Technol.,* IS&T, Springfield, VA, 1995, p. 349.
12. H. Endert, R. Pätzel and D. Basting, *Optical and Quantum Electronics* **27**, 1319 (1995).
13. B. Galéa, J. Xing, R. Gaglione, P. Attané and A. Soucemarianadin, *IS&T's 9th Intl. Cong. on Advances in Non Impact Printing Technol.*, IS&T, Springfield, VA, 1993, p. 282.
14. Lord Rayleigh, *Proc. Roy. Soc. Lond.* **29**, 71 (1879).
15. Lord Rayleigh, *Phil. Mag.* **34**, 145 (1892).
16. C. Weber, *ZAMM* **11**, 136 (1931).
17. J. B. Keller, S. I. Rubinow and Y. O. Tu, *Phys. Fluids* **16**, 2052 (1973).
18. S. J. Leib and M. E. Goldstein, *J. Fluid Mech.* **168**, 479 (1986).
19. H. H. Taub, *Phys. Fluids* **19**, 1124 (1976).
20. R. Fagerquist, *IS&T's 11th Intl. Cong. on Advances in Non Impact Printing Technol.*, IS&T, Springfield, VA, 1995, p. 362.